J. Fluid Mech. (2010), *vol.* 663, *pp.* 53–69.
doi:10.1017/S002211201000337X

On liquid films on an inclined plate

E. S. BENILOV[1]†, S. J. CHAPMAN[2], J. B. MCLEOD[2], J. R. OCKENDON[2] AND V. S. ZUBKOV[1]

[1]Department of Mathematics and Statistics, University of Limerick, Limerick, Ireland

[2]Mathematical Institute, 24–29 St Giles', Oxford OX1 3LB, UK

(Received 3 September 2009; revised 21 June 2010; accepted 21 June 2010; first published online 18 August 2010)

This paper examines two related problems from liquid-film theory. Firstly, a steady-state flow of a liquid film down a pre-wetted plate is considered, in which there is a precursor film in front of the main film. Assuming the former to be thin, a full asymptotic description of the problem is developed and simple analytical estimates for the extent and depth of the precursor film's influence on the main film are provided. Secondly, the so-called drag-out problem is considered, where an inclined plate is withdrawn from a pool of liquid. Using a combination of numerical and asymptotic means, the parameter range where the classical Landau–Levich–Wilson solution is not unique is determined.

Key words: coating, interfacial flows (free surface), lubrication theory

1. Introduction

Liquid films have been studied for several decades, but in spite of the collective effort of many researchers, a number of important questions remain open.

One such question is associated with *precursor films*, which occur, for example, in the problem of the spreading of drops on a pre-wetted substrate. Precursor films are often introduced 'artificially' when simulating flows involving contact lines, such as, for example, spreading of drops on a dry substrate. As a result, instead of solving the governing equations in a domain bounded by the contact line, one can deal with a fixed domain, which is incomparably simpler. Such an approach, however, requires one to carefully monitor the extent to which the 'main' film is affected by the precursor film.

There is a large body of literature published on precursor films, with two papers being directly relevant to this study. Voinov (1977) calculated the characteristics of the transition region between the main and precursor films; however, his results are not applicable to the former and, thus, do not allow one to see if it was affected by the latter. Tuck & Schwartz (1990), in turn, considered a thin layer flowing down a pre-wetted wall; having computed numerically the solution describing the main film, they matched it to Voinov's asymptotic solution in the transition region. However, no analytical estimates of the precursor film's effect on the main film were obtained.

In §§ 2 and 3 of this study, we consider a liquid film steadily flowing down a pre-wetted sloping substrate. Assuming that the precursor film is much thinner than the main film, we develop a full asymptotic description of the problem and thus provide

† Email address for correspondence: eugene.benilov@ul.ie

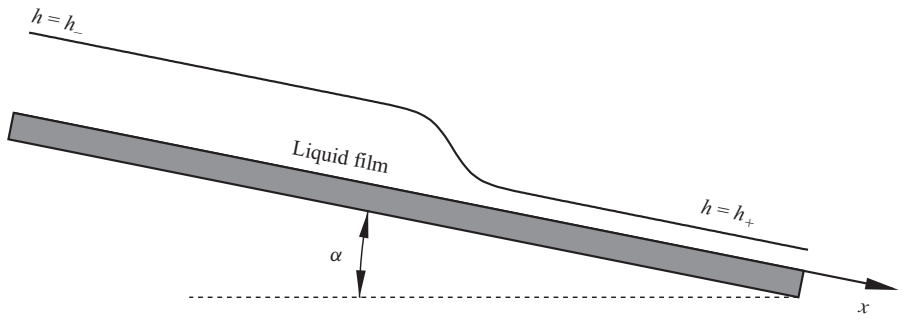

FIGURE 1. A liquid film flowing down an inclined substrate. h_+ and h_- are the thickness of the precursor film and the main film, respectively.

simple estimates for the extent and depth of the precursor film's influence on the main film.

Another open question in liquid-film theory is associated with the so-called drag-out problem, where an inclined plate is withdrawn from a pool of liquid and one needs to calculate the thickness of the film clinging to the plate. For a vertical plate, this setting was examined by Landau & Levich (1942); Wilson (1982) then extended their results to a plate inclined at an arbitrary angle. More recent results, however, indicate that the Landau–Levich–Wilson (LLW) solution is not unique, as instances of non-LLW solutions have been computed by Jin, Acrivos & Münch (2005) and Snoeijer *et al.* (2008). Also they have been observed experimentally by the latter group of authors, who argued that the LLW solution corresponds to the idealized limit of a perfectly wetting liquid, while non-LLW solutions describe the general case of non-perfectly wetting liquids and, thus, are crucially important physically. Finally, an equivalent of non-LLW solutions was computed by Münch & Evans (2005) and Evans & Münch (2006) for a similar setting involving a pool of liquid and an inclined plate (which, however, was at rest, but the film was still driven up the slope by the Marangoni effect).

In §§ 4 and 6 of this study, we examine the parameter space of the drag-out problem and, using a combination of numerical and asymptotic methods, determine the region in the problem's parameter space where non-LLW solutions exist. We shall find that the drag-out and precursor-film problems have many common features, due to which we consider them together.

2. The precursor-film problem: formulation

Consider a liquid film flowing down an inclined plate as in figure 1, and let ρ, ν and σ be the liquid's density, kinematic viscosity and surface tension, respectively; α is the angle between the substrate and the horizontal, and g is the acceleration due to gravity. We are interested in flows where the film surface has a 'smoothed-shock' profile, translating down the plate with a fixed velocity (say, V). To make the profile stationary, it is convenient to assume that the plate is moving in the opposite direction with the same velocity.

Under the lubrication approximation, a steady-film flow on an inclined plate moving with a velocity $-V$ is described by (e.g. Wilson 1982)

$$-Vh_* + \frac{h_*^3}{3}\left(\frac{g\sin\alpha}{\nu} - \frac{g\cos\alpha}{\nu}\frac{\mathrm{d}h_*}{\mathrm{d}x_*} + \frac{\sigma}{\rho\nu}\frac{\mathrm{d}^3h_*}{\mathrm{d}x_*^3}\right) = -q, \tag{2.1}$$

where x_* and h_* are the spatial coordinate and the film thickness, respectively, the asterisks imply that the corresponding variables are dimensional and $-q$ is the liquid flux (where the minus sign is introduced for convenience). Note that the term $g\sin\alpha$ describes the down-the-slope acceleration, the term $g\cos\alpha$ describes the hydrostatic pressure gradient due to variations of the film's thickness, and the terms involving V and σ are the plate's motion and surface tension, respectively. Note that the lubrication approximation requires that the slope of the film surface be small, so that

$$\frac{H}{X} \ll 1, \tag{2.2}$$

where H and X are the characteristic thickness of the film and its horizontal scale, respectively.

To non-dimensionalize the problem, introduce

$$x = \frac{x_*}{X}, \quad h = \frac{h_*}{H}. \tag{2.3}$$

When dealing with the precursor-film problem, it is convenient to set

$$X = \left(\frac{\sigma H}{\rho g \sin\alpha}\right)^{1/3}, \quad H = \left(\frac{V\nu}{g\sin\alpha}\right)^{1/2}, \tag{2.4}$$

after which (2.1) becomes

$$-h + \frac{h^3}{3}\left(1 - \beta\frac{\mathrm{d}h}{\mathrm{d}x} + \frac{\mathrm{d}^3h}{\mathrm{d}x^3}\right) = -\varepsilon, \tag{2.5}$$

where

$$\varepsilon = \frac{q}{VH}, \tag{2.6}$$

is the non-dimensional flux and

$$\beta = \frac{H}{X\tan\alpha}, \tag{2.7}$$

is the ratio of the slope of the film surface to that of the plate. We shall assume the latter to be of order one, so that $\tan\alpha = O(1)$; together with condition (2.2), this makes β negligible. As a result, (2.5) can be reduced to

$$-h + \frac{h^3}{3}\left(1 + \frac{\mathrm{d}^3h}{\mathrm{d}x^3}\right) = -\varepsilon. \tag{2.8}$$

This equation is to be solved with the following boundary conditions:

$$h \to h_\pm \quad \text{as} \quad x \to \pm\infty, \tag{2.9}$$

where h_- and h_+ are the thicknesses of the main and precursor film, respectively. It can be proved (Benilov, Benilov & O'Brien 2009) that a solution to the boundary-value problem (2.8)–(2.9) exists only if

$$h_- \geqslant h_+. \tag{2.10}$$

Finally, it follows from (2.8)–(2.9) that $h_\pm$ are related to ε by

$$-h_\pm + \tfrac{1}{3}h_\pm^3 = -\varepsilon. \tag{2.11}$$

This equality should be treated as an equation for $h_\pm$ and, as such, should have two positive roots satisfying condition (2.10). In the limit of small ε, (2.11) yields

$$h_- = 3^{1/2} + O(\varepsilon), \quad h_+ = \varepsilon + O(\varepsilon^3) \quad \text{as} \quad \varepsilon \to 0. \tag{2.12}$$

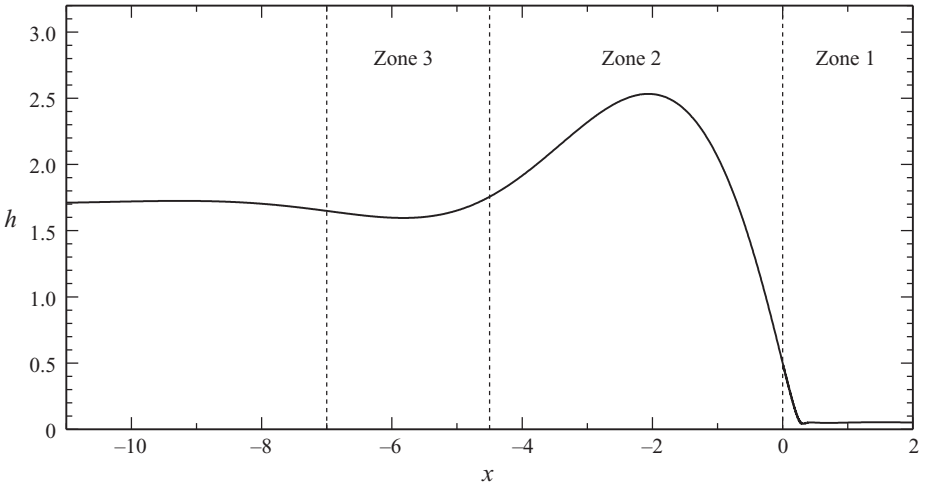

FIGURE 2. A typical solution of the boundary-value problem (2.8)–(2.11), computed numerically for $h_+ = 0.05$ (which corresponds to $\varepsilon \approx 0.049958$).

Thus, if the precursor film is thin, its non-dimensional thickness can be identified with the non-dimensional flux ε.

3. The precursor-film problem: analysis

In this section, the boundary-value problem (2.8)–(2.9) will be examined in the limit $\varepsilon \to 0$.

3.1. *Asymptotic results*

A typical numerical solution of the exact boundary-value problem is shown in figure 2. Observe that it has the shape of a smoothed shock, with a 'bulge' at its front and a small 'trough' behind it.

It is convenient to number the asymptotic zones from right to left (see figure 2).

Zone 1 is the transition region between the bulge on its left and the thin film on its right, and it is described by the equation used by Voinov (1997) (it had also arisen in a similar problem considered by Landau & Levich 1942). Following these two papers, we assume

$$x = \varepsilon x_1, \quad h = \varepsilon h_1, \tag{3.1}$$

after which (2.8) yields, to leading order,

$$-h_1 + \frac{h_1^3}{3}\frac{\mathrm{d}^3 h_1}{\mathrm{d}x_1^3} = -1. \tag{3.2}$$

The right-hand boundary condition follows from (2.9) and (2.12), and is

$$h_1 \to 1 \quad \text{as} \quad x_1 \to +\infty, \tag{3.3}$$

whereas, on the left, h_1 has three possible asymptotic behaviours (Hocking 1990)

$$h_1 \to 1 \qquad \text{as} \quad x_1 \to -\infty, \tag{3.4a}$$

$$h_1 \sim C x_1^2 \qquad \text{as} \quad x_1 \to -\infty, \tag{3.4b}$$

$$h_1 \sim -x_1 \left[9 \ln(-x_1)\right]^{1/3} \quad \text{as} \quad x_1 \to -\infty, \tag{3.4c}$$

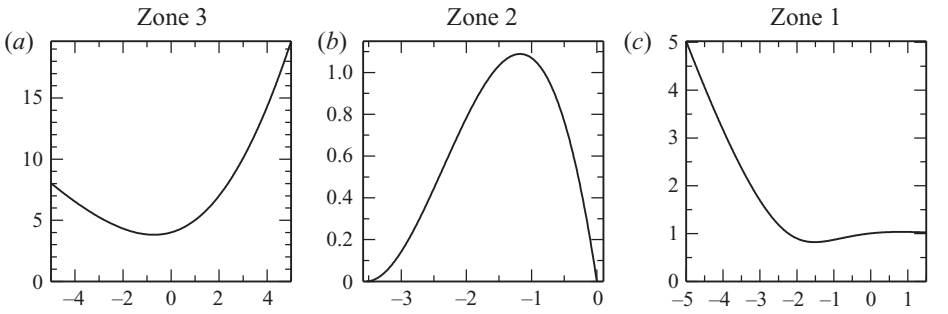

FIGURE 3. The solutions in the first three asymptotic zones for the precursor-film problem.

where $C \neq 0$ is an undetermined constant. It turns out that the only asymptotic behaviour that matches the solution in zone 2 (to be presented below) is (3.4*c*).

The solution of the boundary-value problem (3.2)–(3.4*c*) has been computed by Tuck & Schwartz (1990), and it is shown in figure 3(*c*).

The scaling in zone 2 is

$$x = \gamma^{-1/6} x_2, \quad h = \gamma^{-1/2} h_2, \tag{3.5}$$

where γ is a small parameter such that

$$\gamma = O(|\ln \varepsilon|^{-1}); \tag{3.6}$$

a specific convenient value will be assigned to γ later. Then, (2.8) becomes

$$-\gamma h_2 + \frac{h_2^3}{3}\left(1 + \frac{\mathrm{d}^3 h_2}{\mathrm{d}x_2^3}\right) = -\varepsilon \gamma^{3/2}, \tag{3.7}$$

which, to leading order, yields

$$1 + \frac{\mathrm{d}^3 h_2}{\mathrm{d}x_2^3} = 0. \tag{3.8}$$

The general solution of this equation is

$$h_2 = -\tfrac{1}{6}(x_2 + w)(x_2 + v)(x_2 + u), \tag{3.9}$$

where $u \leqslant v \leqslant w$ are constants of integration. Matching with zone 1 gives

$$u = 0. \tag{3.10}$$

We shall distinguish the cases $v \neq w$ and $v = w$, corresponding to linear or quadratic asymptotics of h_2 as $x_2 \to -v$. It turns out that the former cannot be matched to the zone 3 solution, thus, we assume

$$v = w, \tag{3.11}$$

and solution (3.9)–(3.11) becomes

$$h_2 = -\tfrac{1}{6}(x_2 + w)^2 x_2, \tag{3.12}$$

where w can be interpreted as the width of the bulge.

Finally, to determine w and the scaling parameter γ, the asymptotic behaviour of h_2 as $x_2 \to 0$ should be matched to the asymptotic behaviour of h_1 as $x_1 \to -\infty$, which yields

$$w = 2^{1/2} 3^{5/6}, \tag{3.13}$$

$$\gamma = [\ln(\varepsilon^{-1} \gamma^{-1/6})]^{-1}. \tag{3.14}$$

The latter equation relates γ to ε; it can be shown that

$$\gamma = |\ln \varepsilon|^{-1} + O\left(\frac{\ln|\ln\varepsilon|}{|\ln\varepsilon|^2}\right), \tag{3.15}$$

which validates our original estimate that γ is *logarithmically* small in ε. The solution (3.12)–(3.13) is shown in figure 3(*b*).

The scaling in zone 3 is

$$x = -W + \gamma^{1/6} x_3, \quad h = \gamma^{1/6} h_3, \tag{3.16}$$

where $W = w\gamma^{-1/6}$ is the non-scaled equivalent of the scaled width w of the bulge. Then, (2.8) becomes

$$-h_3 + \frac{h_3^3}{3}\left(\gamma^{1/3} + \frac{\mathrm{d}^3 h_3}{\mathrm{d}x_3^3}\right) = -\varepsilon\gamma^{-1/6}, \tag{3.17}$$

which, to leading order, yields

$$-h_3 + \frac{h_3^3}{3}\frac{\mathrm{d}^3 h_3}{\mathrm{d}x_3^3} = 0. \tag{3.18}$$

To match h_3 to solution (3.12)–(3.13) in zone 2, we require

$$h_3 \sim 2^{-1/2} 3^{-1/6} x_3^2 \quad \text{as} \quad x_3 \to +\infty. \tag{3.19}$$

To complete the asymptotic solution of the problem, we should require that

$$h_3 \to 3^{1/2}\gamma^{-1/6} \quad \text{as} \quad x_3 \to -\infty \tag{3.20}$$

(which corresponds to $h \to h_-$ as $x \to -\infty$), but, unfortunately, none of solutions of (3.18) satisfies (3.20). Thus, we need to introduce another pair of zones (zones 4 and 5, respectively) to the left of zone 3, which mirror zones 2 and 3, respectively.

To match zone 3 to zone 4, we require

$$h_3 \sim -x_3[9\ln(-x_3)]^{1/3} \quad \text{as} \quad x_3 \to -\infty. \tag{3.21}$$

The solution of the boundary-value problem (3.18)–(3.21) is shown in figure 3(*a*): it describes the trough located behind the bulge at the front of the shock, similar to the problem described by Benilov, Benilov & Kopteva (2008).

The scaling and all other characteristics of zones 4 and 5 can be obtained from those of zones 2 and 3 by replacing γ with a doubly logarithmically small parameter $\delta = O[(\ln|\ln\varepsilon|)^{-1}]$, related to γ by

$$\delta = [\ln(\gamma^{-1}\delta^{-1/6})]^{-1}, \tag{3.22}$$

which is, essentially, the same equation that relates γ to ε, as seen by comparing (3.22) with (3.14). Since zone 5 is simply a re-scaled version of zone 3, we again have the problem that the boundary condition at $-\infty$ cannot be satisfied. Thus, two further zones (zones 6 and 7) need to be introduced, similar to zones 2 and 3, but with a *triply* logarithmically small parameter. This series of asymptotic zones continues indefinitely. Similar problems with an infinite number of asymptotic zones were previously considered by Wilson & Jones (1983), Duchemin, Lister & Lange (2005) and Benilov *et al.* (2008).

3.2. *Can the infinite series of asymptotic zones be combined?*

In each of our series of asymptotic zones the small parameter is the logarithm of the previous zone's small parameter. It is tempting to try and formulate a uniform

approximation in which both order 1 and logarithmically small terms are retained, which would take the place of the infinite series of zones.

Consider, for example, zone 3 but retaining the $O(\gamma^{1/3})$ term in (3.17), but still omitting the smaller, $O(\epsilon)$, term, which gives

$$-h_3 + \frac{h_3^3}{3}\left(\gamma^{1/3} + \frac{\mathrm{d}^3 h_3}{\mathrm{d}x_3^3}\right) = 0. \tag{3.23}$$

The solution of (3.23) contains all the logarithmic terms of the original expansion (in zone 3), and is consistent with the global boundary condition at minus infinity,

$$h_3 \to 3^{1/2}\gamma^{1/6} \quad \text{as} \quad x_3 \to -\infty. \tag{3.24}$$

However, the new term alters the asymptotics of h_3 at plus-infinity: instead of quadratic, it becomes cubic with

$$h_3 \sim -\tfrac{1}{6}\gamma^{1/3}x_3^3 \quad \text{as} \quad x_3 \to +\infty; \tag{3.25}$$

this behaviour cannot be matched to solution (3.12) in zone 2. A similar mismatch occurs if one retains the $O(\gamma)$ term in zone 2 (3.7).

Thus, we have been unable to find a single uniformly valid equation, and are left with an infinite series of zones with sequentially increasing small parameter. The question of how such a solution can be used for practical purposes is addressed in § 3.3.

3.3. *Physical interpretation of the asymptotic results*

Mathematically, the most unusual feature of the problem at hand is the infinite number of asymptotic zones. These zones can be interpreted as capillary ripples, with even-numbered zones describing the crests and odd-numbered zones describing the troughs. However, only a few of these zones are 'visible' in, say, a numerical solution computed for a small, but finite ε (see Tuck & Schwartz 1990, figures 2 and 5). Only the first three zones can be typically observed, with the most important one being zone 2 describing the bulge. Then, using formulae (3.12), (3.13) and (3.5), we can estimate the height and width of the bulge as

$$\max\{h(x)\} \approx 2^{5/2}3^{-3/2}\gamma^{-1/2}, \tag{3.26}$$

$$W \approx 2^{1/2}3^{5/6}\gamma^{-1/6}, \tag{3.27}$$

where γ is related to ε by (3.14) (recall that ε is the non-dimensional thickness of the precursor film). Expressions (3.26) and (3.27) describe the extent and depth of the precursor film's influence on the main film. Note that they both grow as the precursor film becomes thinner.

We recall that precursor films are widely used as a means of avoiding domains with variable boundaries when modelling films with contact lines. In such simulations, one can use (3.26) and (3.27) as estimates of the extent and depth of the precursor film's effect on the actual solution and, thus, assess whether the observed dynamics are affected by the introduction of the precursor film.

Finally, in order to test the accuracy of our asymptotic results, formula (3.26) was compared to the solution of the exact problem computed numerically (using the method employed by Benilov *et al.* 2008 for a similar problem). The results are shown in figure 4: one can see that, for $\varepsilon = 10^{-3}$, the asymptotic error is approximately 14 %. (The correction term in zone 2 is $O(\gamma)$; with $\varepsilon = 10^{-3}$, $\gamma \approx 0.138$, so the error of this magnitude is to be expected.) For smaller ε, the accuracy of the numerical method

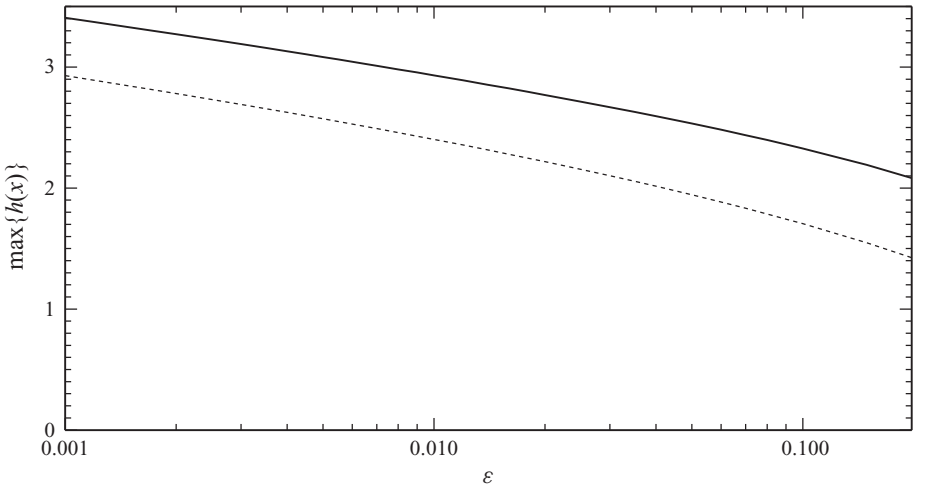

FIGURE 4. The dependence of $\max\{h(x)\}$ on ε for the solution of the boundary-value problem (2.8)–(2.11). The numerical result is the solid line and the dotted line shows the asymptotic result (3.22).

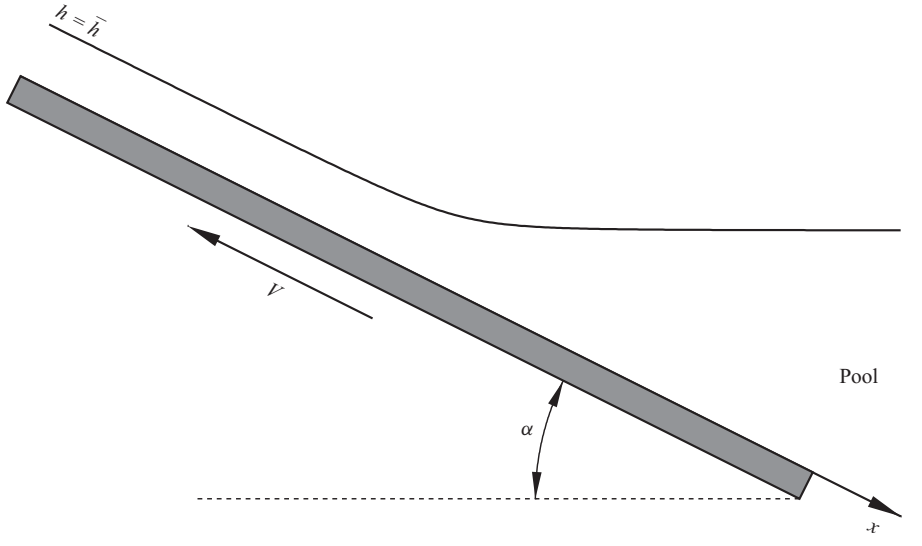

FIGURE 5. The drag-out problem.

rapidly deteriorates, making the asymptotic approach the only reliable method to estimate the precursor film's effect.

4. The drag-out problem: formulation

The drag-out problem will be examined using (2.1), with V being the velocity with which the plate is withdrawn from the pool (see figure 5). This equation, however, will be non-dimensionalized in a different way: instead of (2.4), we shall assume that

the scales for x and h in (2.3) are

$$X = \frac{H^3 g \cos\alpha}{V\nu}, \quad H = \left(\frac{V\nu}{g\sin\alpha}\right)^{1/2}, \tag{4.1}$$

after which substitution of (2.3) into (2.1) yields

$$-h + \frac{h^3}{3}\left(1 - \frac{\mathrm{d}h}{\mathrm{d}x} + \frac{1}{\varepsilon}\frac{\mathrm{d}^3 h}{\mathrm{d}x^3}\right) = -\varepsilon^{1/6} Q, \tag{4.2}$$

where

$$\varepsilon = \frac{\rho V \nu}{\sigma \tan^3\alpha}, \quad Q = \frac{q}{HV\varepsilon^{1/6}}, \tag{4.3}$$

are the capillary number and the non-dimensional flux (in the latter, the factor $\varepsilon^{1/6}$ has been introduced for convenience). The boundary conditions describing the drag-out problem are

$$h \to \bar{h} \quad \text{as} \quad x \to -\infty, \tag{4.4}$$

$$h \sim x \quad \text{as} \quad x \to +\infty, \tag{4.5}$$

where $\bar{h}$ is the *load* (i.e. the thickness of the film clinging to the plate) and condition (4.5) describes the unperturbed surface of the pool. Observe that $\bar{h}$ and Q are related by

$$-\bar{h} + \frac{\bar{h}^3}{3} = -\varepsilon^{1/6} Q. \tag{4.6}$$

Note that, in the context of the drag-out problem, (4.2) is applicable only if the plate slope is small (for more details, see Benilov & Zubkov 2008).

The difference between the LLW (Landau–Levich–Wilson) and non-LLW solutions is best explained using an argument suggested by Münch & Evans (2005) for a similar problem. Observe that, if $\varepsilon^{1/6} Q < 2/3$, (4.6) has two distinct positive roots for the load $\bar{h}$. In the limit $\varepsilon \to 0$, these roots are

$$\bar{h} = \varepsilon^{1/6} Q + O(\varepsilon^{1/2}) \tag{4.7}$$

and

$$\bar{h} = 3^{1/2} + O(\varepsilon^{1/6}). \tag{4.8}$$

The LLW solution corresponds to the smaller $\bar{h}$ (given by (4.7)), whereas non-LLW solutions correspond to the larger one (given by (4.8)).

The drag-out problem has been considered recently by Snoeijer *et al.* (2008). They demonstrated analytically and experimentally the existence of a one-parameter family of non-LLW solutions (for example parametrized by the load $\bar{h}$). These solutions comprise three asymptotic zones, although only the 'dimple' zone was solved for (it corresponds to our zone 2 (5.11), (5.15)–(5.17) below).

In what follows, we shall present a more detailed analysis of the non-LLW solutions, showing that they actually comprise an infinite series of asymptotic zones as in the precursor-film problem of § 3. Moreover, we shall find that, for a certain region of parameter space, there are multiple non-LLW solutions with the same load.

5. The drag-out problem: results

5.1. *Numerical results*

The boundary-value problem (4.2)–(4.6) was solved numerically via an approach used previously by Münch & Evans (2005).

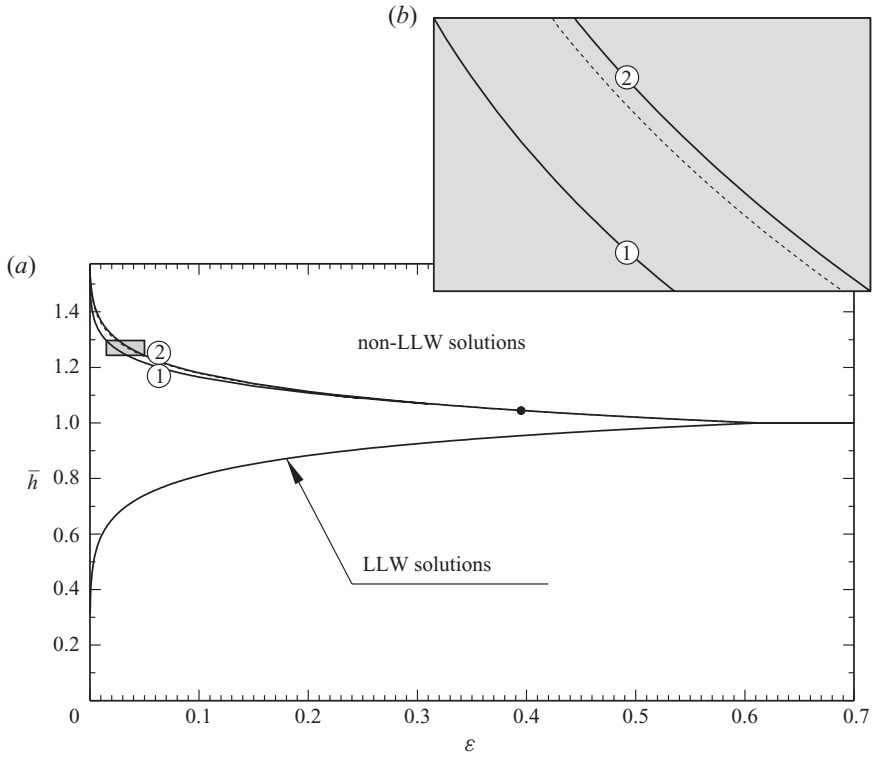

FIGURE 6. The parameter space of the boundary-value problem (4.2)–(4.6): ε is the capillary number, $\bar{h}$ is the load. (*b*) A blow-up of the shaded region in (*a*). The region where non-LLW solutions exist is located above curve (1). The dotted line represents the 'centreline' (defined in (5.2)). Curve (1) separates the subregion with at least two non-LLW solutions from the subregion where no solutions exist. Curve (2) separates the subregions with exactly one and at least three non-LLW solutions. The black dot in (*a*) is the point (5.3) of intersection of all of the above curves.

The best way to represent the solutions found is to consider the $(\varepsilon, \bar{h})$ parameter plane. The LLW solution, for example, corresponds to a *curve*,

$$\bar{h} = \bar{h}^{(L)}(\varepsilon), \tag{5.1}$$

whereas non-LLW solutions occupy a *region* (see figure 6*a*). Observe that, at $\varepsilon \approx 0.6$, the curve merges into the boundary of the region; not surprisingly, this occurs when the flux is $\varepsilon^{1/6} Q = 2/3$ and the two roots of (4.6) coalesce onto $\bar{h} = 1$. For $\varepsilon \gtrsim 0.6$, the boundary of the region where solutions exist appears to be very close to $\bar{h} = 1$ (see figure 6*a*).

For most points of the non-LLW region, a single solution exists for each pair $(\varepsilon, \bar{h})$, but there are also subregions where two, three or more solutions can be found.

To describe these subregions, it is convenient to introduce a curve on the $(\varepsilon, \bar{h})$ plane corresponding to the solution with same flux as that of the LLW solution, but corresponding to a different $\bar{h}$, such that

$$-\bar{h} + \tfrac{1}{3}\bar{h}^3 = -\bar{h}^{(L)} + \tfrac{1}{3}\left(\bar{h}^{(L)}\right)^3, \quad \bar{h} \neq \bar{h}^{(L)}. \tag{5.2}$$

In the following, curve (5.2) will be referred to as the 'centreline', and in figure 6(*b*)

it is shown as dotted. Generally, the centreline is located close to the boundary of the non-LLW region and intersects it at some point (shown in figure 6 by a black dot).

In the area far above the centreline, where $\bar{h}$ is large, only a single solution exists, but closer to the centreline, in a narrow strip, at least three solutions can be found; in figure 6, the curve separating the regions with exactly one and at least three solutions is marked with a circled 2. In an even narrower strip above the centreline, so narrow that it is invisible in figure 6, five solutions can be found, etc.

Below the centreline, in turn, there is a strip where at least two solutions can be found; in figure 6, the boundary between this strip and the region with no solutions is marked with a circled 1. In a narrower strip closer to, and still below, the centreline, at least four solutions exist, etc.

The above observations suggest that, at the centreline itself, the number of solutions is infinite, and this conjecture will be supported by asymptotic evidence in § 5.2. Also note that all the curves mentioned above appear to converge to the same point (see figure 6),

$$\varepsilon \approx 0.395, \quad \bar{h} \approx 1.045, \tag{5.3}$$

so the region with multiple LLW solutions is located to the left of this point.

Finally, examples of non-LLW solutions with coincident pairs $(\varepsilon, \bar{h})$ are shown in figure 7(*b*), and the LLW solution for the same ε is shown in figure 7(*a*). One can see that, before settling at the expected value of $\bar{h}$ as $x \to -\infty$, non-LLW solutions oscillate about a smaller value, $\bar{h}^{(L)}$, which corresponds to the LLW solution with the same ε. Generally, non-LLW solutions with the same $\bar{h}$ differ from each other by the number of oscillations about $\bar{h}^{(L)}$ (see figure 7*b*).

5.2. *Analytical results*

In § 5.2, we shall examine non-LLW solutions under the assumption

$$\varepsilon \ll 1, \tag{5.4}$$

corresponding to the limit of strong surface tension (the opposite limit $\varepsilon \gg 1$ has been examined earlier by Derjaguin (1943) and Benilov & Zubkov (2008)). First we shall briefly re-work Wilson's (1982) result (which was obtained using a more general approach, not assuming the plate's slope to be small). Then we shall explain how the asymptotic scheme should be modified to obtain non-LLW solutions.

5.2.1. *The Landau–Levich–Wilson solution*

To derive the equivalent of the LLW solution, two asymptotic zones need to be considered: one for the pool and another for the film (see figure 8*a*). The former is described by the following variables:

$$x = \varepsilon^{-1/2} x_1, \quad h = \varepsilon^{-1/2} h_1. \tag{5.5}$$

Substituting (5.5) into (4.2), (4.5) and omitting small terms, we obtain

$$1 - \frac{\mathrm{d}h_1}{\mathrm{d}x_1} + \frac{\mathrm{d}^3 h_1}{\mathrm{d}x_1^3} = 0, \tag{5.6}$$

$$h_1 \sim x_1 \quad \text{as} \quad x_1 \to +\infty. \tag{5.7}$$

To match the pool solution $h_1(x_1)$ to the thin-film solution in the next zone, we

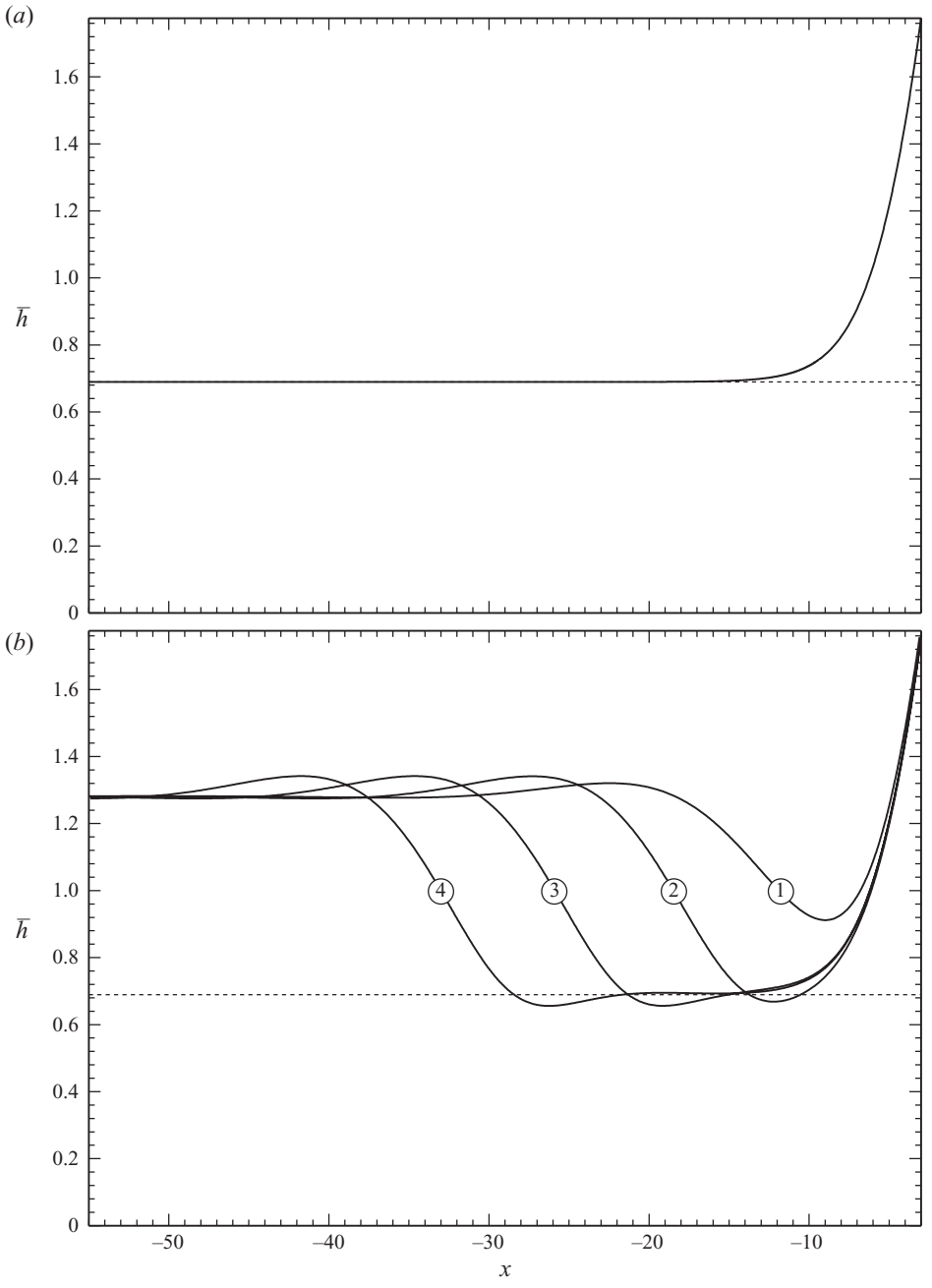

FIGURE 7. Numerical solutions of the boundary-value problem (4.2)–(4.6) with $\varepsilon = 0.03$: (*a*) the LLW solution; (*b*) non-LLW solutions (computed for $\bar{h} = 1.28112$). The dotted line corresponds to $\bar{h}^{(L)}$.

require

$$h_1 = 0, \quad \frac{\mathrm{d}h_1}{\mathrm{d}x_1} = 0 \quad \text{at} \quad x_1 = 0. \tag{5.8}$$

The boundary-value problem (5.6)–(5.8) can be readily solved to give

$$h_1 = x_1 + \mathrm{e}^{-x_1} - 1. \tag{5.9}$$

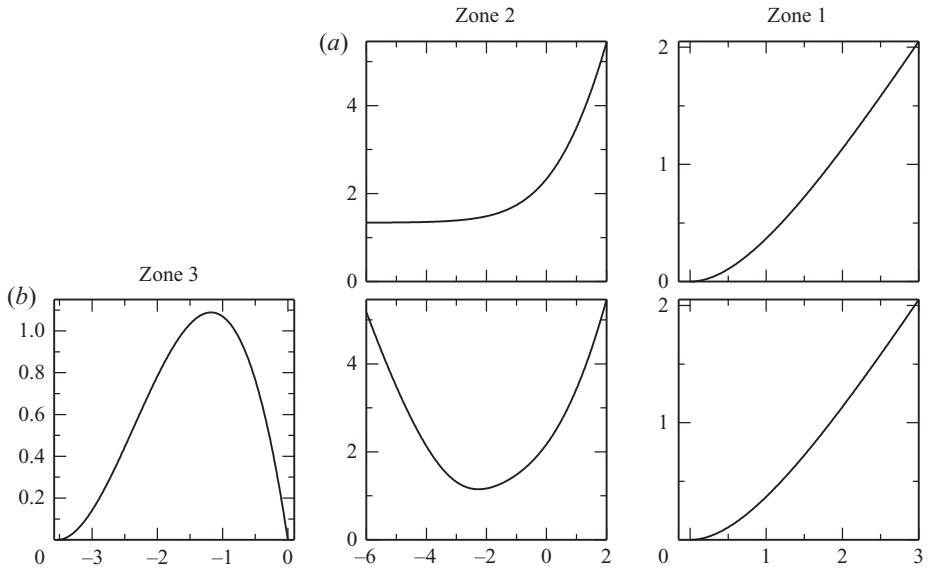

FIGURE 8. The structure of the asymptotic solution of the drag-out problem. (*a*) The LLW solution. (*b*) The first three zones for non-LLW solutions.

In the next zone (describing the film), the scaling is

$$x = \varepsilon^{-1/6} x_2, \quad h = \varepsilon^{1/6} h_2, \tag{5.10}$$

after which (4.2)–(4.4), (4.6) and (4.7) yield, to leading order,

$$-h_2 + \frac{h_2^3}{3}\frac{\mathrm{d}^3 h_2}{\mathrm{d}x_2^3} = -Q, \tag{5.11}$$

$$h_2 \to Q \quad \text{as} \quad x_2 \to -\infty. \tag{5.12}$$

It can be verified by inspection that, to match h_2 to h_1, one should require

$$h_2 \sim \tfrac{1}{2} x_2^2 \quad \text{as} \quad x_2 \to +\infty. \tag{5.13}$$

As shown by Landau & Levich (1942), Bretherton (1961) and Wilson (1982), the boundary-value problem (5.11)–(5.13) does not have a solution, unless Q assumes a certain value. To understand why, consider the limit $x_2 \to -\infty$ where $h_2 \approx Q$ and (5.11) can be linearized about Q. Using the linearized (5.11), one can show that, after satisfying the boundary condition (5.12), the solution contains only one arbitrary constant corresponding to shifting the coordinate, $x_2 \to x_2 + \text{const}$. Accordingly, to satisfy the other boundary condition, (5.13), one has to adjust Q, which can be viewed as an 'eigenvalue' of the boundary-value problem (5.11)–(5.13). In the following, this specific value of Q will be denoted by $Q^{(L)}$.

The solution of (5.11)–(5.13) can be readily computed resulting in

$$Q^{(L)} \approx 1.3376. \tag{5.14}$$

The corresponding zone 2 solution $h_2(x_2)$ is shown in figure 9(*a*).

5.2.2. *Non-LLW solutions*

The first asymptotic zone in this case is the same as that for the LLW solution and is described by (5.5) and (5.9). For zone 2, the old scaling, (5.10), again remains

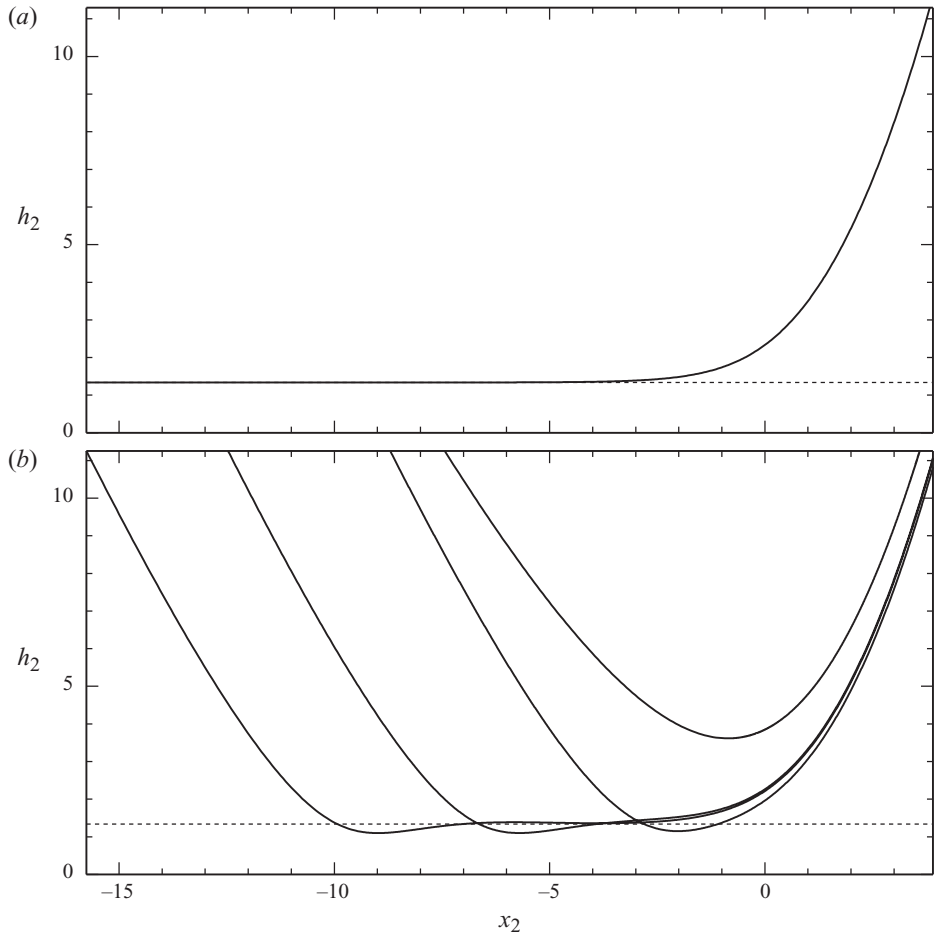

FIGURE 9. Examples of solutions of the boundary-value problem (5.11), (5.15)–(5.17). The dotted line corresponds to $h_2 = \bar{h}^{(L)}$. (*a*) The LLW solution and (*b*) non-LLW solutions (all computed for $Q = 1.3376 \approx Q^{(L)}$).

appropriate, as well as (5.11) and the right-hand boundary condition (5.13). The left-hand condition, however, is different, as the solution should increase with decreasing x and, eventually, approach its load (which is now of the order 1 – see (4.8)). Accordingly, instead of (5.12), we shall require h_2 grow with x_2 as

$$h_2 \sim -x_2[9\ln(-x_2)]^{1/3} \quad \text{as} \quad x_2 \to -\infty. \tag{5.15}$$

Closer inspection of (5.11) reveals that

$$h_2 \sim \tfrac{1}{2}x_2^2 + bx_2 + a \quad \text{as} \quad x_2 \to \infty, \tag{5.16}$$

where b and a are constants. We can eliminate b by shifting the x_2-axis and, thus, obtain

$$h_2 \sim \tfrac{1}{2}x_2^2 + a \quad \text{as} \quad x_2 \to \infty. \tag{5.17}$$

In this case, it is the undetermined constant a that plays the role of an eigenvalue: when 'shooting' the solution from $+\infty$, a needs to be adjusted to satisfy the boundary conditions at $-\infty$.

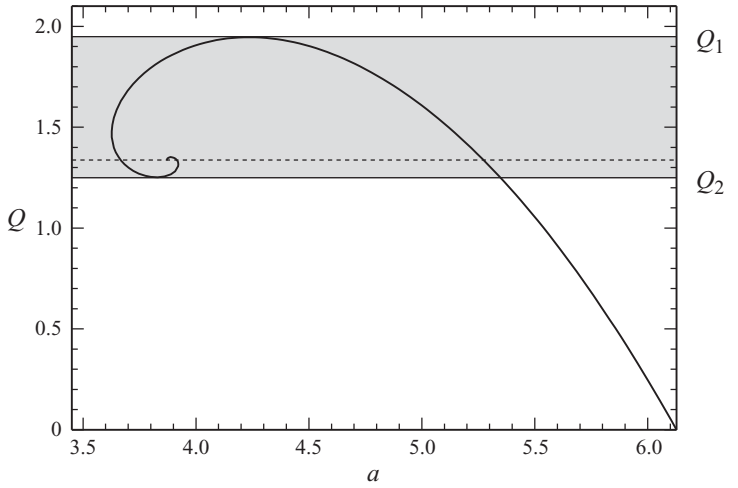

FIGURE 10. The relationship between a and Q, as determined by the boundary-value problem (5.11), (5.15)–(5.17). The dotted line shows the LLW value of the flux, $Q = Q^{(L)}$. The region where solution is non-unique is shaded.

The boundary-value problem (5.11), (5.15)–(5.17) describing zone 2 is the key to understanding the non-uniqueness of non-LLW solutions. It was previously considered by Snoeijer *et al.* (2008), who found numerically a unique solution for each value of Q, and these solutions gave a good fit with experimental data. They did not match this solution to the 'film region', where the film thickness approaches its limiting value, $\bar{h}$.

We point out that the solution of (5.11), (5.15)–(5.17) cannot match directly into the film region, but must proceed through an infinite series of asymptotic zones as in § 3. More importantly, the boundary-value problem (5.11), (5.15)–(5.17) does not always have a unique solution (for given Q), but may have multiple solutions.

The key to understanding the origin of this multiplicity is the relationship between Q and a, which has been computed numerically and is shown in figure 10. One can see that, for $Q > Q_1 \approx 1.946$, no solutions exist; for $Q < Q_2 \approx 1.251$, one solution exists; for $Q \in (Q_3, Q_1)$ (where $Q_3 \approx 1.352$), two solutions exist; etc. Note that our value of Q_1 corresponds to the limiting value of Q computed by Snoeijer *et al.* (2008) for the existence of non-LLW solutions (the numeric values of the two constants differ by a factor of $\sqrt{2}$ due to different non-dimensionalizations).

If we let Q_j be the value of Q where the number of solutions changes from $j-1$ to $j+1$, then figure 10 suggests that the sequence Q_j converges to $Q^{(L)}$. As a result, the number of solutions tends to infinity as $Q \to Q^{(L)}$, and by changing Q, the number of solutions of the boundary-value problem (5.11), (5.15)–(5.17) can be made arbitrarily large. Although this argument is based on numerical evidence, it can be proved rigorously; this will be the subject of a forthcoming paper.

We have also computed examples of solutions of (5.11), (5.15)–(5.17), which are shown in figure 9(b). Comparing figure 9 with figure 7, where numerical solutions of the exact problem are shown, one can see that the asymptotic solutions bear many of the characteristic features of the exact ones, including the presence of an interval where they oscillate about the LLW load $\bar{h}^{(L)}$.

The rest of the drag-out problem is similar to the precursor-film problem and, thus, will not be discussed in detail. To illustrate the similarity, consider zone 3 of the

former case: the scaling and solution there can be shown to be

$$x = \varepsilon^{-1/3}\gamma^{-1/6}x_3, \quad h = \gamma^{-1/2}h_3, \tag{5.18}$$

$$h_3 = -\tfrac{1}{6}(x_3 + w)^2 x_3, \tag{5.19}$$

where γ and w satisfy

$$\gamma^{-1} = \ln(\varepsilon^{-1/6}\gamma^{-1}), \quad w = 2^{1/2}3^{5/6}. \tag{5.20}$$

Then, comparing (5.19) with (3.12), one can see that zone 3 of the drag-out problem is similar to zone 2 of the precursor-film problem (both zones describe a bulge). After that, an infinite sequence of alternating troughs and bulges follow, just as they did in the precursor-film problem.

6. Summary and concluding remarks

In this paper, two problems from the liquid-film theory have been examined.

Firstly, we considered a liquid layer flowing down a sloping plate, under the condition that the main film is preceded by a thin precursor film. A full asymptotic description of the flow has been obtained, revealing some unusual features such as the infinite number of asymptotic zones. It has been demonstrated that the solution describing the film is of a smoothed-shock type, with a bulge at the front (see figure 2), the height and width of which are determined by (3.26) and (3.27), respectively.

Note that precursor films are often used in numerical modelling of liquid films, because, by surrounding the main film with a thin precursor film, one can avoid dealing with contact lines. To this end, one can use expressions (3.26) and (3.27) as estimates of the extent and depth of the precursor film's effect on the actual solution and, thus, assess how the observed dynamics are affected by the introduction of the precursor film. Most importantly, as the precursor film's thickness decreases, the extent and depth of its influence actually grow (see (3.26) and (3.27)).

It is worth noting that the analysis presented in § 3 in this paper can be readily modified for a setting where the precursor film is replaced by a contact line. In this case, one only needs to replace the solution in zone 1 (describing the transition region between the 'bulge' and precursor film) with a thin boundary layer describing the region adjacent to the contact line.

Secondly, we considered the drag-out problem, concentrating on solutions with a load larger than that of the LLW solution. Numerically, our main result is figure 6 which shows the region in the problem's parameter space where non-LLW solutions exist, and the subregions with multiple non-LLW solutions. Asymptotically, in the limit of strong surface tension, the multiplicity of non-LLW solutions is a result of non-uniqueness of the solution to the asymptotic boundary-value problem (5.11), (5.15)–(5.17), which describes the film near the edge of the pool. Also note that the case of non-LLW solutions of the drag-out problem includes an infinite number of asymptotic zones and, in this respect, is similar to the precursor-film problem.

Although we have not addressed the issue of stability in this paper, preliminary results suggest that, at least, some of the steady solutions of the drag-out problem are stable. In particular, employing the approach of Evans & Münch (2006), Zubkov (2009) demonstrated that solutions (1) and (3) in figure 7(*b*) are stable, whereas (2) and (4) are unstable. We remark that the stability of smoothed-shock solutions can also be examined in the spirit of Bertozzi *et al.* (1998, 2001) (see also Bertozzi & Shearer 2000; Segin, Tilley & Kondic 2005).

One of the authors (E.S.B.) is grateful for the hospitality of the Oxford Centre for Collaborative Applied Mathematics which hosted his sabbatical, and also acknowledges the support of the Science Foundation Ireland (RFP Grant 08/RFP/MTH1476 and Mathematics Initiative Grant 06/MI/005). This publication was based on work supported in part by Award No. KUK-C1-013-04 , made by King Abdullah University of Science and Technology (KAUST).

REFERENCES

Benilov, E. S., Benilov, M. S. & Kopteva, N. 2008 Steady rimming flows with surface tension. *J. Fluid Mech.* **597**, 81–118.

Benilov, E. S., Benilov, M. S. & O'Brien, S. B. G. 2009 Existence and stability of regularized shock solutions, with applications to rimming flows. *J. Engng Maths* **63**, 197–212.

Benilov, E. S. & Zubkov, V. S. 2008 On the drag-out problem in liquid-film theory. *J. Fluid Mech.* **617**, 283–299.

Bertozzi, A. L., Münch, A., Fanton, X. & Cazabat, A. M. 1998 Contact line stability and "Undercompressive Shocks" in driven thin film flow. *Phys. Rev. Lett.* **81**, 5169–5172.

Bertozzi, A. L., Münch, A., Shearer, M. & Zumbrun, K. 2001 Stability of compressive and undercompressive thin film travelling waves. *Eur. J. Appl. Maths* **12**, 253–291.

Bertozzi, A. L. & Shearer, M. 2000 Existence of undercompressive traveling waves in thin film equations. *SIAM J. Math. Anal.* **32**, 194–213.

Bretherton F. P. 1961 The motion of long bubbles in tubes. *J. Fluid Mech.* **10**, 166–188.

Derjaguin, B. 1943 Thickness of liquid layer adhering to walls of vessels on their emptying and the theory of photo- and motion-picture film coating. *C. R. (Dokl.) Acad. Sci. URSS* **39**, 13–16.

Duchemin, L., Lister, J. R. & Lange, U. 2005 Static shapes of levitated viscous drops. *J. Fluid Mech.* **533**, 161–170.

Evans, P. L. & Münch, A. 2006 Interaction of advancing fronts and meniscus profiles formed by surface-tension-gradient-driven liquid films. *SIAM J. Appl. Maths* **66**, 1610–1631.

Hocking, L. M. 1990 Spreading and instability of a viscouse fluid sheet. *J. Fluid Mech.* **211**, 373–392.

Jin, B., Acrivos, A. & Münch, A. 2005 The drag-out problem in film coating. *Phys. Fluids* **17**, 103603.

Landau, L. & Levich, B. 1942 Dragging of liquid by a plate. *Acta Physiochim USSR* **17**, 42–54.

Münch, A. & Evans, P. L. 2005 Marangoni-driven liquid films rising out of meniscus onto a nearly horizontal substrate. *Physica* D **209**, 164–177.

Segin, T. M., Tilley, B. S. & Kondic, L. 2005 On undercompressive shocks and flooding in countercurrent two-layer flows. *J. Fluid Mech.* **532**, 217–242.

Snoeijer, J. H., Ziegler J., Andreotti B., Fermigier M., & Eggers J. 2008 Thick films of viscous fluid coating a plate withdrawn from a liquid reservoir. *Phys. Rev. Lett.* **100**, 244502.

Tuck, E. O. & Schwartz, L. W. 1990 A numerical and asymptotic study of some third-order ordinary differential equations relevant to draining and coating flows. *SIAM Rev.* **32**, 453–469.

Voinov, O. V. 1977 Inclination angles of the boundary in moving liquid layers. *J. Appl. Mech. Tech. Phys.* **18**, 216–222.

Wilson, S. D. R. 1982 The drag-out problem in film coating theory. *J. Engng Maths* **16**, 209–221.

Wilson, S. D. R. & Jones, A. F. 1983 The entry of a falling film into a pool and the air-entrainment problem. *J. Fluid Mech.* **128**, 219–230.

Zubkov, V. S. 2009 On the drag-out problem in liquid film theory. PhD Thesis, University of Limerick, Limerick, Ireland.